

Human adipose-derived stem cells preconditioned with a novel herbal formulation Jing Shi attenuate doxorubicin-induced cardiac damage

Dennis Jine-Yuan Hsieh^{1,2}, Bruce Chi-Kang Tsai³, Parthasarathi Barik³, Marthandam Asokan Shibu⁴, Chia-Hua Kuo^{5,6}, Wei-Wen Kuo^{7,8}, Pi-Yu Lin⁹, Cheng-Yen Shih¹⁰, Shinn-Zong Lin^{11,12}, Tsung-Jung Ho^{12,13,14,*}, Chih-Yang Huang^{3,15,16,17,18,*}

¹School of Medical Laboratory and Biotechnology, Chung Shan Medical University, Taichung, Taiwan

²Clinical Laboratory, Chung Shan Medical University Hospital, Taichung, Taiwan

³Cardiovascular and Mitochondrial Related Disease Research Center, Hualien Tzu Chi Hospital, Buddhist Tzu Chi Medical Foundation, Hualien, Taiwan

⁴Department of Biotechnology, Bharathiar University, Coimbatore, India

⁵Laboratory of Exercise Biochemistry, University of Taipei, Taipei, Taiwan

⁶Department of Kinesiology and Health Science, College of William and Mary, Williamsburg, VA 23187, USA

⁷Department of Biological Science and Technology, China Medical University, Taichung, Taiwan

⁸Ph.D. Program for Biotechnology Industry, China Medical University, Taichung, Taiwan

⁹Buddhist Compassion Relief Tzu Chi Foundation, Hualien, Taiwan

¹⁰Buddhist Tzu Chi Medical Foundation, Hualien, Taiwan

¹¹Department of Neurosurgery, Hualien Tzu Chi Hospital, Hualien, Taiwan

¹²Integration Center of Traditional Chinese and Modern Medicine, Hualien Tzu Chi Hospital, Buddhist Tzu Chi Medical Foundation, Hualien, Taiwan

¹³Department of Chinese Medicine, Hualien Tzu Chi Hospital, Hualien, Taiwan

¹⁴School of Post-Baccalaureate Chinese Medicine, College of Medicine, Tzu Chi University, Hualien, Taiwan

¹⁵Department of Medical Research, China Medical University Hospital, China Medical University, Taichung, Taiwan

¹⁶Department of Medical Laboratory Science and Biotechnology, Asia University, Taichung, Taiwan

¹⁷Center of General Education, Buddhist Tzu Chi Medical Foundation, Tzu Chi University of Science and Technology, Hualien, Taiwan

¹⁸Graduate Institute of Basic Medical Science, China Medical University, Taichung City, Taiwan

*Equal contribution

Correspondence to: Chih-Yang Huang; email: cyhuang@mail.cmu.edu.tw

Keywords: cardiac hypertrophy, reactive oxygen species, autophagy, Chinese herbal medicine, adipose-derived stem cells

Received: May 15, 2023

Accepted: August 21, 2023

Published: September 13, 2023

Copyright: © 2023 Hsieh et al. This is an open access article distributed under the terms of the [Creative Commons Attribution License](https://creativecommons.org/licenses/by/3.0/) (CC BY 3.0), which permits unrestricted use, distribution, and reproduction in any medium, provided the original author and source are credited.

ABSTRACT

Pathological cardiac hypertrophy is a considerable contributor to global disease burden. Chinese herbal medicine (CHM) has been used to treat cardiovascular diseases since antiquity. Enhancing stem cell-mediated recovery through CHM represents a promising approach for protection against doxorubicin (Dox)-induced cardiac hypertrophy. Herein, we investigated whether human adipose-derived stem cells (hADSCs) preconditioned with novel herbal formulation Jing Si (JS) improved protective ability of stem cells against doxorubicin-induced cardiac damage. The effect of JS on hADSC viability and migration capacity was determined via MTT and migration assays,

respectively. Co-culture of hADSC or JS-preconditioned hADSCs with H9c2 cells was analyzed with immunoblot, flow cytometry, TUNEL staining, LC3B staining, F-actin staining, and MitoSOX staining. The *in vivo* study was performed M-mode echocardiography after the treatment of JS and JS-preconditioned hADSCs by using Sprague Dawley (SD) rats. Our results indicated that JS at doses below 100 µg/mL had less cytotoxicity in hADSC and JS-preconditioned hADSCs exhibited better migration. Our results also revealed that DOX enhanced apoptosis, cardiac hypertrophy, and mitochondrial reactive oxygen species in DOX-challenged H9c2 cells, while H9c2 cells co-cultured with JS-preconditioned hADSCs alleviated these effects. It also enhanced the expression of autophagy marker LC3B, mTOR and CHIP in DOX-challenged H9c2 cells after co-culture with JS-preconditioned hADSCs. In Dox-challenged rats, the ejection fraction and fractional shortening improved in DOX-challenged SD rats exposed to JS-preconditioned hADSCs. Taken together, our data indicate that JS-preconditioned stem cells exhibit a cardio-protective capacity both *in vitro* and *in vivo*, highlighting the value of this therapeutic approach for regenerative therapy.

INTRODUCTION

Epidemiological studies have shown that pathological cardiac hypertrophy is a major cause of morbidity and mortality worldwide. Pathological cardiac hypertrophy causes sudden heart failure, accounting for up to 17.3 million deaths annually [1]. In developed countries, hypertrophy-associated heart failure is typically associated with several risk factors, including stress, aging, diet, and physical inactivity [2, 3]. Chronic cardiac hypertrophy causes several cardiovascular conditions, including hypertension, ischemic disease, and heart failure [4]. Hypertrophy involves enhanced cardiac remodeling to increase left ventricular mass, causing left ventricular hypertrophy [5]. Doxorubicin (Dox), an effective anthracycline chemotherapeutic, is widely used in the treatment of several cancers, including lung, breast, prostate, and bone cancer, as well as leukemias [6]. However, various studies indicate that Dox can induce cardio toxicity inside and outside the cell by causing lipid peroxidation outside cardiomyocytes and free radical generation, organelle damage, and cellular signal imbalances inside cardiomyocytes, affecting heart function [6]. Furthermore, elevated Dox levels can cause cardiac hypertrophy leading to detrimental effects, such as cardiomegaly [7–9]. Typically, Dox causes excessive oxidative damage to the heart, promoting apoptosis [10]. Dox also has adverse effects on cytoplasmic calcium homeostasis [11]. Myocardial inflammation is driven by the activation of nuclear factor kappa B, a major transcription factor within the inflammatory response, and is also induced by Dox [12]. Transcription factor p53 is involved in upstream events leading to activation of the apoptotic pathway in mitochondria during Dox-induced cardiomyocyte death [13]. Developing novel therapies to reduce Dox cardiotoxicity is essential for improving its clinical efficacy.

Chinese herbal medicine is an effective and reliable treatment for several diseases [14, 15], and are widely used in various parts of the world. Importantly, CHM

treatment is associated with few side effects [16, 17]. Owing to its high efficacy, few side effects, and low cost, CHM has been the focus of extensive research on cancer, cardiovascular diseases, diabetes, and coronavirus infectious disease (COVID-19), as well as stem cell therapy [18]. The novel herbal formulation Jing Si (JS) is used as tea in Taiwan. It contains various bioactive compounds and exhibits pharmacological properties that might protect cells under stress [19]. For instance, JS reduces DOX-related hypertrophic effects and DNA damage in H9c2 cells. It also enhances autophagic clearance in MPP-damaged SH-SY5Y neuroblasts. In addition, JS was shown to favorably regulate metabolism in a type II diabetes animal model. The growth of different cancer cell lines was suppressed by JS treatment. Further, JS was shown to promote stem cell homeostasis and offers cellular protection [19]. JS is composed of eight different CHM herbs and contains polyphenols, alkaloids, amino acids, organic acids, coumarins, vitamins, and phenols, which together act to exert beneficial effects on the human body.

Mesenchymal stem cell transplantation is an emerging approach in the field of regenerative medicine and influences growth factor secretion in cardiovascular disease [20, 21]. However, maintaining stemness alongside cardioprotective function is a major challenge after transplantation into the host. Adipose-derived stem cells (ADSCs) are an attractive option for stem cell therapy to regulate cardiac remodeling, as they are easily obtainable and have multi-lineage differentiation potential [22, 23]. ADSCs are able to regulate the “stem cell niche” in the host by stimulating the recruitment of endogenous stem cells to the transplant site and accelerating their differentiation. ADSCs may also act as free radical scavengers as well as a source of antioxidants and chaperone/heat shock proteins at sites of ischemia or injury [24]. This allows for detoxification of the microenvironment during stress conditions, which supports the remaining cells at these sites [24]. ADSCs also suppress the immune response

and transfer healthy mitochondria to regulate aerobic metabolism. Compared to other stem cell types, ADSCs have notable advantages, such as their availability and low cost. They also secrete various growth factors, including hepatocellular growth factor (HGF), vascular endothelial growth factor (VEGF), insulin-like growth factor (IGF), and platelet-derived growth factor (PDGF), which confer cardioprotective effects under pathological conditions [25].

While Dox is an effective chemotherapeutic agent, its cardiotoxicity contributes to patient mortality. A limited number of studies have examined the effects of CHM on mesenchymal stem cell therapy for cardiac hypertrophy. While JS can promote stem cell homeostasis, there is no evidence to support whether it can enhance stem cell function. Therefore, we aimed to investigate whether JS could enhance the protective effects of ADSCs against Dox-induced cardiotoxicity *in vitro* and *in vivo*. We evaluated the effects of JS on human adipose-derived stem cells (hADSCs) via MTT and migration assays. Co-culture of hADSCs and H9c2 was followed by western blot, flow cytometry, TUNEL staining, immunoblot, F-actin staining, LC3B staining, and MitoSOX staining. For our *in vivo* study, Sprague-Dawley (SD) rats were subjected to M-mode echocardiography after receiving hADSCs. Our findings indicated that JS preconditioning improved the cardioprotective properties of stem cells against Dox, highlighting its value in regenerative therapy.

MATERIALS AND METHODS

Preparation and characterization of Jing Si herbal drink

The Jing Si herbal drink included 6 g of *Ohwia caudate* leaves, 6 g of *Artemisia argyi* leaves, 2 g of *Perilla frutescens* leaves, 4 g of *Ophiopogon japonicas* leaves, 4 g of *Platycodon grandifloras* roots, 4 g of *Houttuynia cordata* (*Ophiopogonis Radix*) roots, 2 g of *Glycyrrhiza uralensis* (*Glycyrrhizae radix*) roots, and 0.2 g of *Chrysanthemum × morifolium* flowers. All herbs were bought from the local herbal store (Hualien, Taiwan) and finely powdered. The herbal mixture was added to 500 mL reverse osmosis water and concentrated to 50 mL via boiling. The preparation was spun down (slow speed) to remove the pellet and then filtered through a 0.45- μ m filter [26].

hADSCs and H9c2 cell culture

hADSCs were purchased from Thermo Fisher (Waltham, MA, USA) and cultured in mesenPRO RSTM basal medium supplemented with mesenPRO RSTM growth factor supplement (Thermo Fisher) in an

incubator at 37° C and 5% CO₂. Cells were sub-cultured once the initial confluency reached 70%, with cells at passage 8 used for the experiments. H9c2 cells were obtained from American Type Culture Collection (USA) and cultured in Dulbecco's Minimum Essential Medium (D5523, Sigma, Saint Louis, MO, USA) containing 10% fetal bovine serum (FBS) (Hyclone, Logan, UT, USA) with 1% penicillin-streptomycin (Invitrogen, Carlsbad, CA, USA), maintained at 37° C in a 5% CO₂ incubator [27].

Co-culture experiment

This method has been described in our previous report [28]. Briefly, hADSCs cultured in mesenPRO RSTM basal medium supplemented with mesenPRO RSTM growth factor supplement were seeded in the upper chamber of a hanging insert (Millipore, Bedford, MA, USA) and placed into the six-well culture plates containing H9c2 cells without contact to the lower chamber. H9c2 cells were cultured in six-well culture dishes. H9c2 cells cultured in Dulbecco's Minimum Essential Medium containing 10% FBS with 1% penicillin-streptomycin were treated with Dox (1 μ M), which was purchased from Sigma-Aldrich and diluted in dimethyl sulfoxide, for 24 h. After incubation for 24h, then cells were washed with PBS three times. The upper chamber with hADSCs preconditioned with JS was inserted into a 6-well dish for co-culture for 24 h. Finally, co-cultured H9c2 cells were washed with PBS three times and used for further experiments.

MTT assay

The hADSCs cells were seeded at a density of 2 x10⁵ cells per well in 24-well plates. The cells were then treated with various concentrations (100–1,000 μ g/mL) of JS for 24 h. MTT reagent (Sigma-Aldrich, Saint Louis, MO, USA) was added at a concentration of 0.5 mg/mL for 4 h at 37° C. The medium was then discarded, and dimethyl sulfoxide was added for solubilization. Finally, the absorbance at 570 nm was measured using an automated microplate reader [29, 30].

Western blot analysis

This method has been described in our previous reports [31–33]. Briefly, protein samples were extracted from H9c2 cells or heart tissues after treatment with lysis buffer (Tris-base [pH 7.4, 50 mM], EDTA [1 M], NaCl [0.5 M], beta-mercaptoethanol [1 mM], NP-40 [1%], IGEPAL CA-630 (Sigma-Aldrich), 10% glycerol, and protease inhibitor cocktail tablets (Roche, New York, NY, USA). Proteins were quantified, and an equal amount of protein from each sample was separated using sodium dodecyl sulphate–polyacrylamide gel electrophoresis. The proteins

were then transferred onto polyvinylidene difluoride membranes (Millipore, Bedford, MA, USA), which were incubated with 5% blocking buffer for 1 h. The membranes were incubated with primary antibodies (mTOR [#2983] and p53 [#2524] from Cell Signaling (Danvers, MA, USA), CHIP [sc-66830] and β -actin [sc-47778] from Santa Cruz Biotechnology, Santa Cruz, CA, USA) at 4° C overnight. Finally, the membranes were incubated with secondary antibodies (horseradish peroxidase-conjugated anti-rabbit and mouse (Santa Cruz Biotechnology, Santa Cruz, CA, USA) for 1 h at 25° C, and antibody binding was visualized using ECL western blotting luminal reagent (Santa Cruz Biotechnology) and the LAS-4000 mini (GE Healthcare Life Sciences) machine [34–36]. All chemicals were purchased from Sigma-Aldrich (St. Louis, MO, USA).

F-actin, mitoSOX, and TUNEL staining

H9c2 cells were cultured in eight-well chamber slides (Greiner Bio-One, Monroe, NC, USA). After reaching 70% confluence, the cells were fixed with 4% paraformaldehyde at room temperature for 1 h, washed thrice with PBS, and permeabilized with 0.1% Triton X-100 for 2 min. The cells were then incubated with rhodamine-phalloidin (Invitrogen), MitoSOX Red reagent (Invitrogen, Carlsbad, CA, USA), and TUNEL reagent (Roche Applied Science, Indianapolis, IN, USA), according to the manufacturer's protocol. After incubation, the cells were washed three times with PBS and counter-stained with DAPI (Abcam, Cambridge, UK) for 15 min for the nucleus staining. The whole field of vision was characterized using a fluorescence magnifying instrument (IX71, Olympus, Tokyo, Japan) associated with an imaging framework (DP2-BSW, Olympus). The quantification results were further assessed and plotted using GraphPad Prism software.

LC3B staining

H9c2 cells were cultured in eight-well chamber slides (Greiner Bio-One, Monroe, NC, USA). After reaching 70% confluence in DMEM containing 10% FBS, the cells were fixed with 4% paraformaldehyde in 1× PBS for 1 h at room temperature. Permeabilization solution (0.5 mL, 0.1% Triton X-100 in 0.1% sodium citrate) was added to each well on ice for 2 min without shaking. Blocking buffer (2% BSA) was added in each well to avoid non-specific binding. Primary antibody against LC3B (#2775, Cell Signaling Technology, 1:100, 500 μ L) was added to each well and incubated at 4° C for 12 h. Subsequently, diluted fluorescent secondary antibody Alexa Fluor® 488 goat anti-rabbit IgG (A11008, Invitrogen, 1:100, 500 μ L) was added to each well and incubated at 25° C for 1 h. DAPI (500 μ L, 10000× diluted) was added to each well. The

plates were incubated for 30 min at 25° C, in the dark. Finally, after washing with PBS, the cells were observed under fluorescence microscope (IX71, Olympus, Tokyo, Japan).

Animal experiments

The animals were purchased from BioLASCO Taiwan Co., Ltd. (Taipei, Taiwan). Eight-week-old SD rats were maintained under a 12-h light/dark cycle at $55 \pm 10\%$ humidity and $22 \pm 2^\circ$ C, with access to food and water. Healthy SD rats were allocated into five groups ($n = 4$ per group) and treated once every 2 weeks for a total 4 weeks, as follows: (Group I) SD rats (control), (Group II) SD rats treated with Dox (7.5 mg/kg) for 4 consecutive weeks to achieve a total concentration of 30 mg/kg, (Group III) SD rats treated with Dox after oral administration of JS (300 mg/kg), (Group IV) SD rats treated with Dox and JS (50 μ g/mL)-preconditioned hADSCs (1×10^6 cells/rat via tail vein injection), and (Group V) SD rats treated with Dox and JS (100 μ g/mL)-preconditioned hADSCs (1×10^6 cells/rat via tail vein injection). After treatment, heart function was analyzed using M-mode echocardiography before the rats were euthanized. Left ventricular internal end-diastolic dimensions (LVIDd), left ventricular internal end-systolic dimensions (LVIDs), stroke volume (SV), and end diastolic volume (EDV) were examined via echocardiography. Fractional shortening (FS) was determined as per the following formula: $FS (\%) = [(LVIDd - LVIDs) / LVIDd] \times 100$. The ejection fraction (EF) was determined as: $EF (\%) = SV / EDV \times 100$ [37–39]. Thereafter, all animals were euthanized via CO₂ asphyxiation. All hearts were collected and stored at -80° C for further experiments.

Analysis of apoptosis by flow cytometry

Flow cytometry analysis was performed using a double staining Annexin V-FITC and propidium iodide (PI) apoptosis detection kit (BD Biosciences, San Jose, CA, USA), according to the manufacturer's protocol for *in vitro* analysis. After processing using the kit, apoptosis analysis was carried out using a FACS Canto™ system (BD Biosciences) at the FACS Core Facility, Tzu-chi Hospital Research Center, Taiwan. The apoptotic cells were gated ($n=10,000$ cells), and the proportion of apoptotic cells was calculated by adding the numbers of cells in the Q2 (late apoptosis) and Q4 (early apoptosis) quadrants.

Migration assay

A migration assay was performed as previously described [40]. In brief, 2×10^5 cells per well were

seeded into the chambers of Transwell plates in serum-free media, and the lower chamber was filled with 10% FBS as an attractant. The plates were incubated for 24 h at 37° C with 5% CO₂. After treatment, the chamber membrane was treated with 4% paraformaldehyde to fix the cells and stained with crystal violet. Cells that migrated to the lower chamber were observed using an OLYMPUS® BX53 microscope (Tokyo, Japan).

Statistical analysis

All data are expressed as the mean ± standard error of the mean (SEM). Quantifications performed in triplicate were analyzed using one-way ANOVA in Prism GraphPad 5 software. P-values lower than *p <0.05, **p <0.01, and ***p <0.001 were considered statistically significant.

Availability of data and material

The raw data used and/or analyzed during the current study are available from the corresponding author on reasonable request. The authors confirm that the data supporting the findings of this study are available within the article.

Consent for publication

The authors agree with the publication of this paper.

RESULTS

JS-preconditioned hADSCs exerted cytoprotective effects on Dox-challenged H9c2 cells

To evaluate the effect of JS on hADSC viability, we performed an MTT assay. The results indicated that after 24 h of treatment, hADSC viability increased under low doses of JS (25, 50, 100 µg/mL), whereas high doses (up to 800 µg/mL) exhibited low cytotoxicity (Figure 1A). Through transwell migration assay to examine the effect of JS treatment on migration efficiency, we observed that hADSC migration increased in a dose-dependent manner at low dose concentrations of JS (Figure 1B). We consider JS contains various bioactive compounds that may regulate the microenvironment by stimulating cells to secrete soluble trophic factors that regulate stemness, through autocrine and paracrine mechanisms. To determine whether JS-preconditioned hADSCs exert a paracrine effect on Dox-challenged H9c2 cells, we

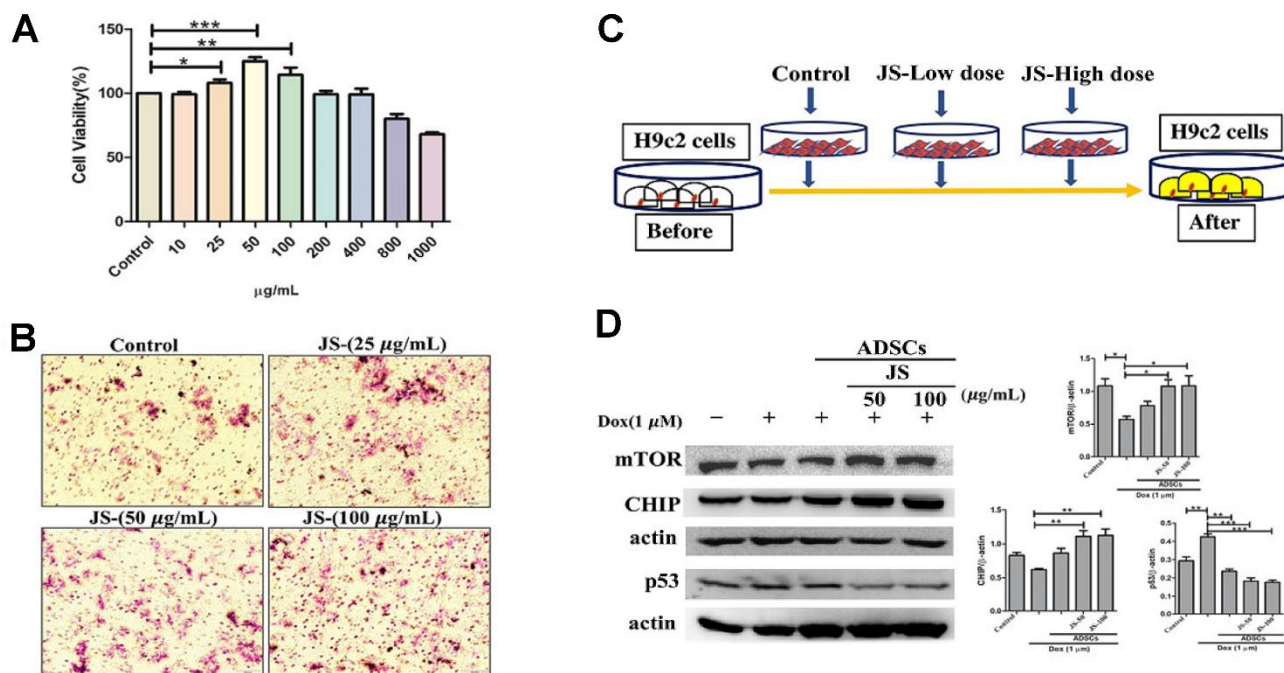


Figure 1. Jing Shi-preconditioned human adipose-derived stem cells (hADSCs) enhanced cytoprotective effects of doxorubicin-challenged H9c2 cells. (A) Cell viability assay indicating cell viability of human adipose-derived stem cells (hADSCs) treated with Jing Shi. (B) Transwell migration assay showing that Jing Shi-preconditioned hADSCs showed more migration efficiency (pink color) compared with that of the control. (C) Schematic diagram outlining the strategy for co-culturing hADSC and doxorubicin-challenged H9c2 cells. (D) Immunoblot results showing that Jing Shi-preconditioned hADSCs co-cultured with doxorubicin-challenged H9c2 cells increased mTOR and CHIP expression and attenuated apoptosis marker p53 protein expression in H9c2 cells. Experiments were performed in triplicate. Data are presented as means ± SEM. *p <0.05, **p <0.01, and ***p <0.001 were considered significant.

performed a co-culture experiment, summarized in a schematic diagram (Figure 1C). The data from western blot analysis revealed that Dox-challenged H9c2 cells exhibited a decreased expression of mammalian target of rapamycin (mTOR) and carboxy terminus Hsp70-interacting protein (CHIP) protein, both of which regulate autophagic flux. Meanwhile, co-culture with hADSCs preconditioned with 50 or 100 $\mu\text{g}/\text{mL}$ JS significantly upregulated mTOR and CHIP in H9c2 cells, while downregulating apoptosis marker p53 in a dose-dependent manner (Figure 1D). Similarly, the autophagic marker LC3B expression in Dox-challenged H9c2 cells was also exhibited lower expression. However, co-culture with hADSCs preconditioned with 50 or 100 $\mu\text{g}/\text{mL}$ JS significantly induced the up-regulated expression and aggregation of LC3B in Dox-challenged H9c2 cells (Figure 2). Because cells utilized autophagy to eliminate protein aggregates and damaged organelles, and by promoting bioenergetic homeostasis [41], these data suggest that JS-preconditioned hADSCs exert a cytoprotective effect to maintain a healthy cellular environment in Dox-challenged H9c2 cells through the stimulation of autophagic mechanism.

JS-preconditioned hADSCs inhibited the apoptosis of Dox-challenged H9c2 cells

Several studies have reported that exposure to Dox promotes apoptosis in H9c2 cells [42, 43]. To

examine whether JS-preconditioned hADSCs protects against Dox-induced apoptosis, we performed flow cytometry analyses of co-cultured H9c2 cells after Annexin V staining. After co-culture of JS-preconditioned hADSCs with H9c2 cells that were treated with Dox for 24 h, we determined the total proportion of apoptotic H9c2 cells by quantifying the number of cells undergoing late apoptosis (upper right quadrant; Q2) and early apoptosis (lower right quadrant; Q4). The apoptotic population was significantly reduced in a dose-dependent manner in Dox-challenged H9c2 cells co-cultured with JS-preconditioned hADSCs, as compared to that following co-culture with untreated ADSCs (Figure 3A, 3B). These data suggest that JS conditioning enhanced stem cell viability, thus maintaining a cytoprotective microenvironment, which helps nullify the cytotoxic effects of Dox exposure in H9c2 cells.

In concordance with the flow cytometry results, we also observed via TUNEL assay that Dox causes apoptosis. Results from TUNEL analyses indicated that the Dox challenge significantly upregulated the number of apoptotic cells, whereas co-culture with JS-preconditioned hADSCs reduced the number of apoptotic cells in a dose-dependent manner (Figure 3C, 3D). Altogether, these results confirm that the JS-preconditioned hADSCs act as a booster to maintain the health of H9c2 cells in response to Dox.

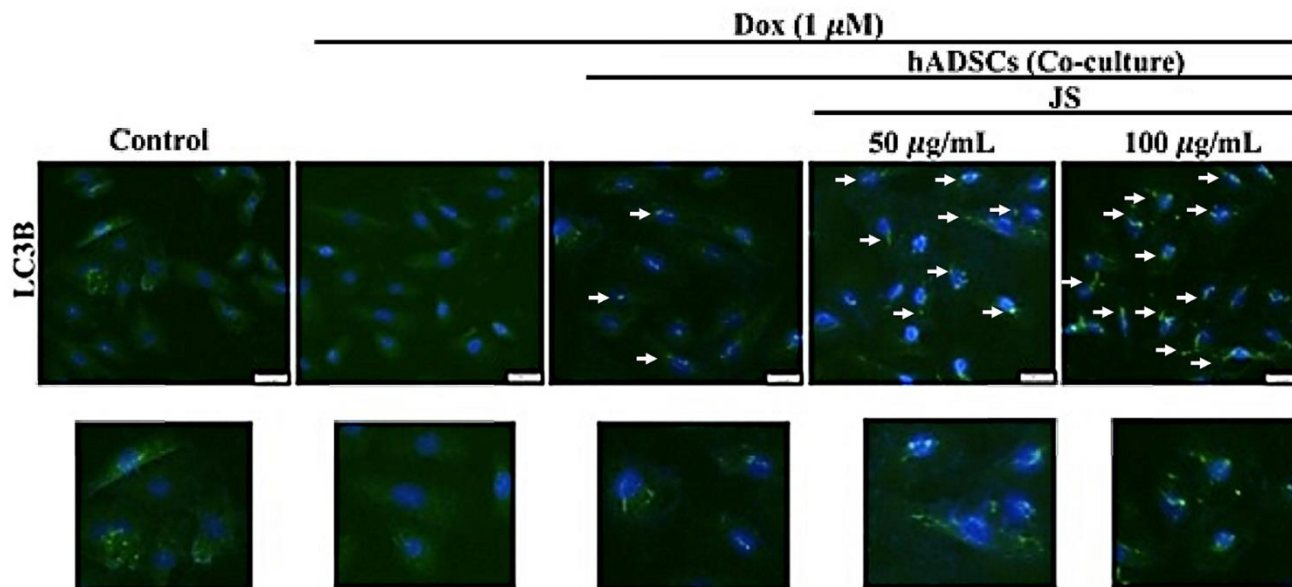


Figure 2. Jing Shi-preconditioned human adipose-derived stem cells (hADSCs) enhanced autophagy of doxorubicin-challenged H9c2 cells. The essential autophagic marker LC3B expression in Dox-challenged H9c2 cells was also exhibited lower expression. However, co-culture with hADSCs preconditioned with 50 or 100 $\mu\text{g}/\text{mL}$ JS significantly induced the upregulated expression of LC3B in H9c2 cells. Scale bar was 100 μm .

JS-preconditioned hADSCs inhibited Dox-induced cellular hypertrophy and mitochondrial ROS generation in H9c2 cells

Dox has been shown to induce hypertrophy in H9c2 cells [44]. Further, prolonged exposure to Dox is associated with reduced heart function, which can lead

to heart failure and sudden cardiac arrest. To validate the hypertrophic response to Dox in H9c2 cells, we performed F-actin staining, the results of which indicated that Dox challenge increased H9c2 cell size, whereas co-culture with hADSCs or JS-preconditioned hADSCs reduced the hypertrophic effects of Dox and normalized the cell size of H9c2 cells. Quantitative

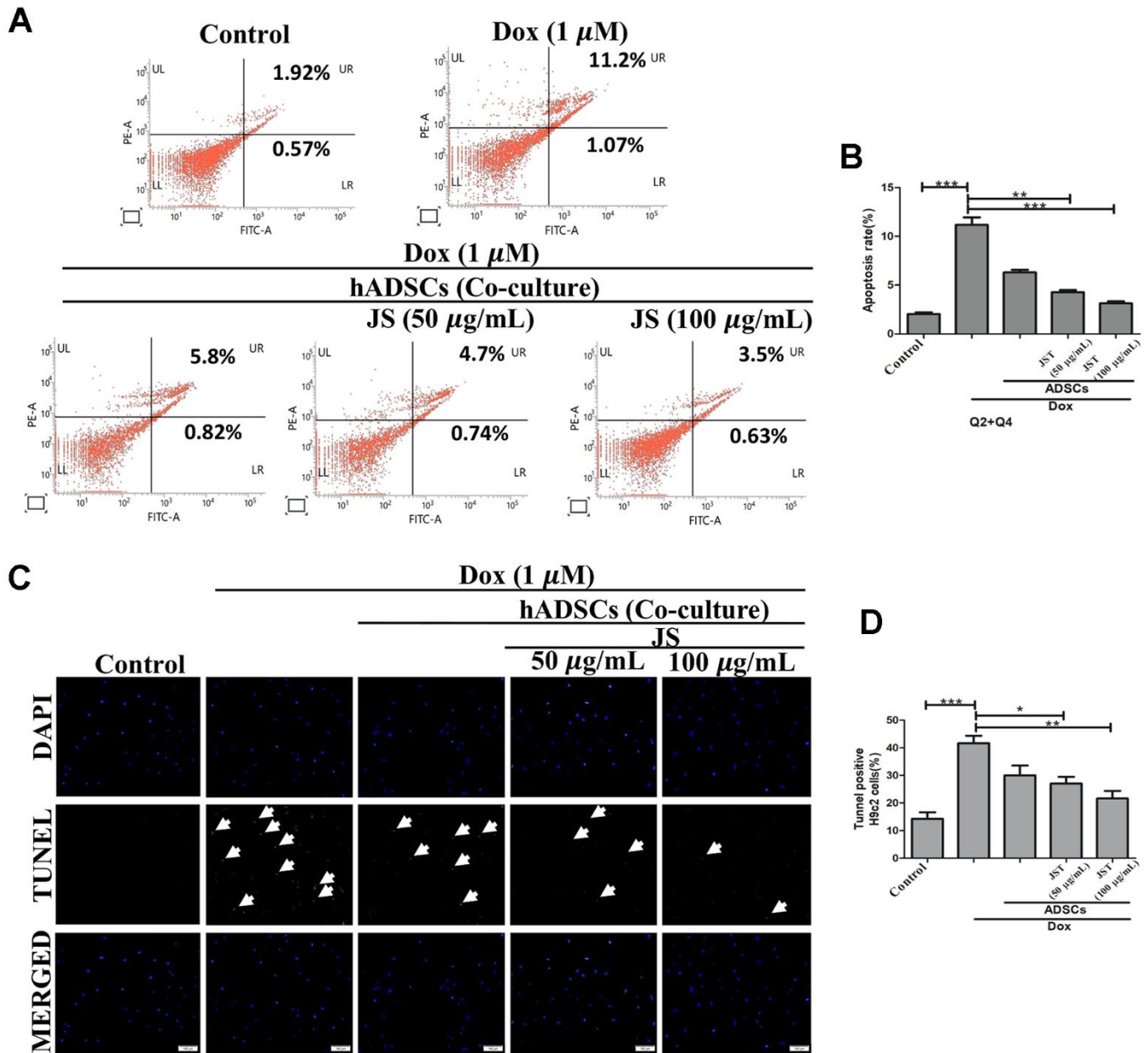


Figure 3. Jing Shi-preconditioned human adipose-derived stem cells (hADSCs) co-cultured with doxorubicin-challenged H9c2 cells decreased doxorubicin-induced apoptosis. (A, B) Flow cytometry analyzing cell apoptosis in H9c2 cells after doxorubicin induction with different JS-preconditioned hADSCs treatment groups versus control. Jing Shi-preconditioned human adipose-derived stem cells (hADSCs) remarkably decreased cell apoptosis in doxorubicin-challenged H9c2 cells **(C, D)** TUNEL assay indicating apoptotic cells (green color fluorescence) in control and different treatment groups. DAPI counter stain indicates the nucleus. The number of TUNEL positive cells decreased when doxorubicin-challenged H9c2 cells were co-cultured with Jing Shi-preconditioned hADSCs. Experiments were performed in triplicate. Data are presented as means \pm SEM. *p < 0.05, **p < 0.01, and ***p < 0.001 were significant.

analysis confirmed that there was a significant increase in H9c2 cells after incubation in Dox for 24 h, but JS-hADSC co-culture significantly had better effect in Dox-treated H9c2 cells and the effect was in a dose-dependent manner (Figure 4A, 4B). Taken together, these findings demonstrated that co-culture with JS-preconditioned hADSCs nullified the hypertrophic response in Dox-treated H9c2 cells.

Dox induces oxidative stress through the generation of reactive oxygen species (ROS) in H9c2 cells [45]. Further, ROS are primarily responsible for the cellular damage and apoptosis associated with Dox exposure. An earlier study showed that increased mitochondrial ROS regulates cardiotoxicity in H9c2 cells [46]. We therefore next to analyze the mitochondrial superoxide generation in JS-treated H9c2 cells challenged with Dox, using MitoSOX red staining. The fluorescence results indicated that Dox enhanced ROS generation, whereas JS-preconditioned hADSCs nullified the increase in ROS in a dose-dependent manner in H9c2 cells (Figure 4C, 4D). Taken together, our data suggest that JS-preconditioned hADSCs exert a neutralizing effect on ROS generated in response to Dox challenge in H9c2 cells.

JS and JS-preconditioned hADSCs regulated cardiac function in Dox-challenged SD rats

The results from our *in vitro* analysis showed that low dose JS enhanced the survival and migration of hADSC. Furthermore, JS-preconditioned hADSCs provide a suitable microenvironment that supports H9c2 cells in nullifying the detrimental effects of Dox. To validate these findings in an *in vivo* model, we next investigated whether JS-preconditioned hADSCs provide cardioprotective effects in Dox-challenged SD rats. Interestingly, we found that both JS and JS-preconditioned hADSCs provided cardioprotective effects to rats challenged with Dox, compared to the only Dox-treated group. The left ventricular internal diameter end diastole (LVIDd) and end systole (LVIDs) values of the JS groups showed a remarkable contractility function after the treatment, with the JS-preconditioned hADSCs exhibited a more pronounced favorable effect (Figure 5A). Similarly, the ejection fraction (EF%) and fractional shortening (FS%) also indicated a significant improvement in cardiac function following JS and JS-hADSC treatment (Figure 5B, 5C). Along with our *in vitro* results, these findings suggest that JS-preconditioned hADSCs could regulate

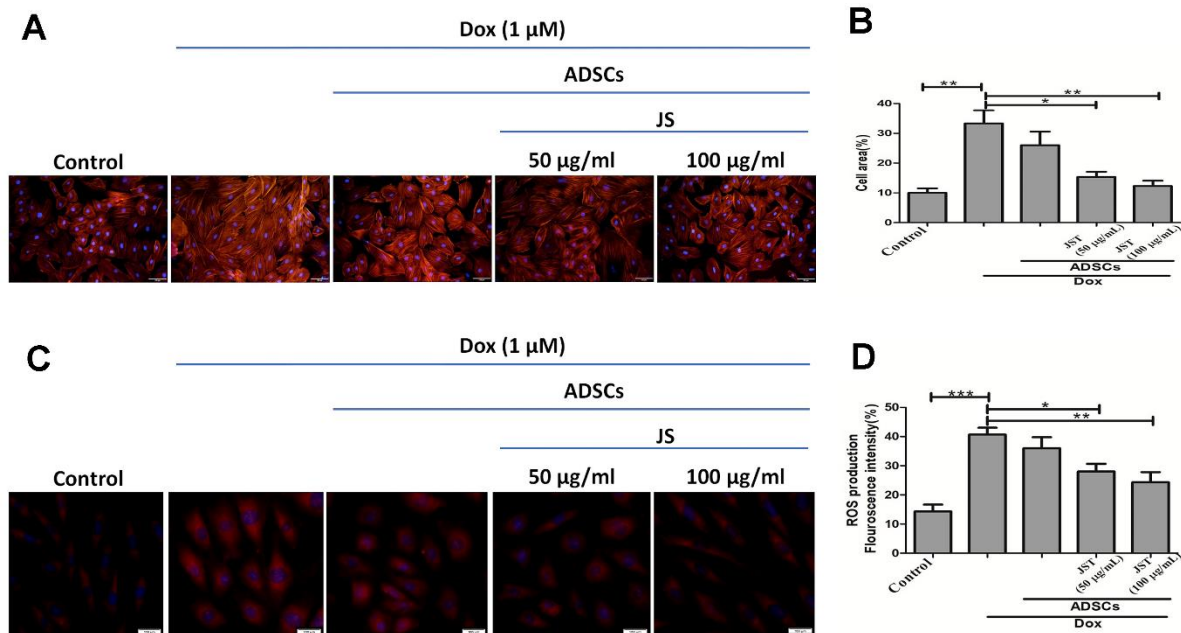


Figure 4. Doxorubicin-challenged H9c2 cells co-cultured with Jing Shi-preconditioned human adipose-derived stem cells (hADSCs) presented less hypertrophy and low-level mitochondrial reactive oxygen species. (A) F-actin staining detecting hypertrophy with or without Doxorubicin induction in H9c2 cells after co-culture with human adipose-derived stem cells (hADSCs). (B) quantitative analysis of cell area for Doxorubicin-challenged H9c2 cells. Jing Shi-preconditioned hADSCs significantly reduced hypertrophy in doxorubicin-challenged H9c2 cells (C, D) MitoSOX staining detecting mitochondrial reactive oxygen species and their quantitative analysis. Doxorubicin-challenged H9c2 cells showed the least mitochondrial reactive oxygen species levels after co-culture with Jing Shi-preconditioned hADSCs. Experiments were performed in triplicate. Data are presented as means \pm SEM. * $p < 0.05$, ** $p < 0.01$, and *** $p < 0.001$ were significant.

mitochondrial ROS and suppress apoptosis to maintain cardiac function following Dox challenge *in vivo*.

DISCUSSION

We have recently demonstrated that resveratrol-preconditioned ADSCs increase the regenerative capacity of diabetic hearts via the Sirt1/Akt signaling pathway [47]. Furthermore, *Alpinia oxyphylla* extract-preconditioned ADSCs attenuate mitochondria-mediated cardiac apoptosis and maintain cardiac function in an aging rat model [48]. Hence, in the current study, we aimed to evaluate the cardioprotective effects of JS-preconditioned hADSCs against Dox-induced cardiac damage and found that JS-preconditioned hADSCs attenuated Dox-induced cardiac damage *in vitro* and *in vivo*.

Autophagy is an important phenomenon that maintains the homeostasis mechanism of the cells during stress conditions. Maintaining autophagic flux via the CHIP and mTOR proteins is an important cellular approach to mimic the experiment with Dox challenge [49]. Previous studies have indicated that Dox challenge causes ROS generation, which leads to cardiac apoptosis via p53 upregulation [44]. Another study also emphasized that Dox attenuated autophagy and co-chaperone activity in SD rats after treatment [50, 51]. Autophagy is an important quality control mechanism

in healthy cells, and its cytoprotective effects involve the removal of unfolded and damaged proteins [52]. Our results identified similar mechanisms, with our *in vitro* data revealed that JS-hADSC treatment against Dox challenge regulated expression of the autophagy marker mTOR and the co-chaperone CHIP, in addition to downregulating the apoptosis marker p53. A previous report shows that CHIP E3 ligase regulates p53 degradation [53] which is in concordance with our western blot analysis. JS may regulate this by its bioactive compounds that leads to maintenance of the mesenchymal stem cells microenvironment, enabling these cells to regulate the secretion of soluble trophic factors and to regulate autophagy in Dox-challenged H9c2 cells. Similarly, JS-hADSC treatment may control mitophagy to reduce apoptosis in Dox-challenged H9c2 cells. For example, Luteolin, a natural compound in vegetables and fruits, activates mitochondrial autophagy to attenuate Dox-induced toxicity in cardiomyocytes [54]. In the present study, mTOR and CHIP expression increased, but p53 expression decreased after co-culture with JS-hADSC. Previous literature mentions that mTOR inhibition immediately changes mitochondrial function [55]. Mitochondrial autophagy is also regulated by CHIP expression and localization [56]. Thus, p53 inhibits Parkin-mediated mitochondrial autophagy resulting in mitochondrial dysfunction [57]. Besides, LC3B is the extensively accepted marker for autophagy activity assessment as it is important for

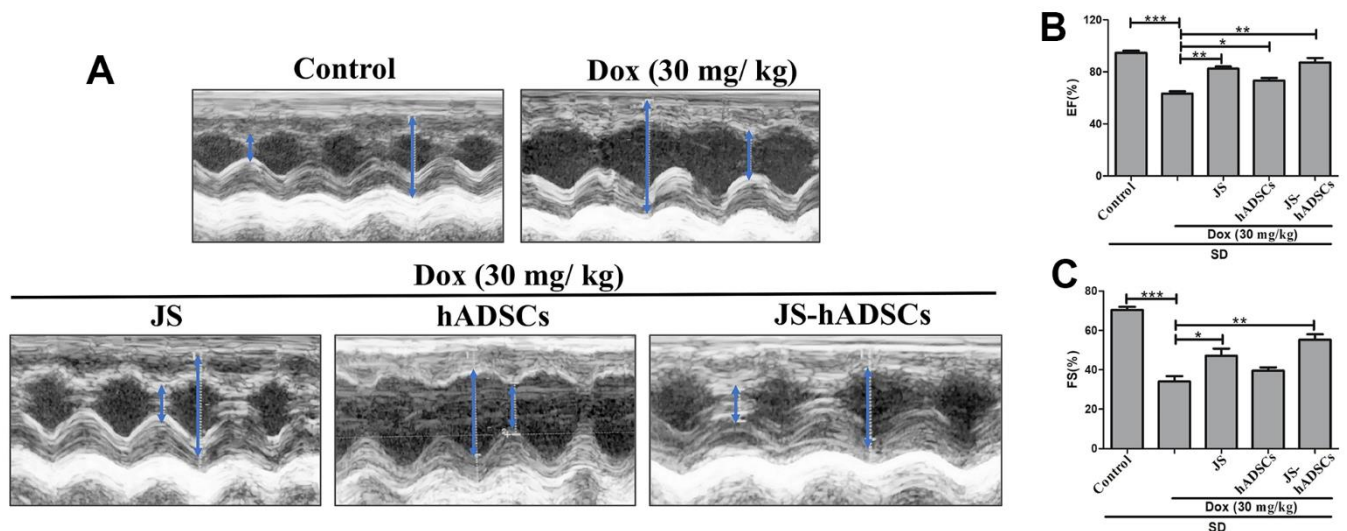


Figure 5. Role of Jing Shi and Jing Shi-preconditioned human adipose-derived stem cells (hADSCs) on cardiac function in doxorubicin-challenged Sprague-Dawley rats. (A) M-mode echocardiography results showing contractility functions (i.e., left ventricular internal diameter end diastole and end systole. (LVIDd and LVIDs)) of all rat groups, indicated by the blue arrow. Doxorubicin-challenged Sprague-Dawley rats treated with Jing Shi-preconditioned human adipose-derived stem cells (hADSCs) showed similar patterns to that of the control group. (B, C) The ejection fraction (EF%) and fractional shortening (FS%) of control, doxorubicin, and various treatment groups. Jing Shi-preconditioned hADSCs showed an improved repair of heart function in Doxorubicin-challenged Sprague-Dawley rats. Experiments were performed in triplicate. Data are presented as means \pm SEM. * $p < 0.05$, ** $p < 0.01$, and *** $p < 0.001$ were significant.

the autophagy mechanism [58]. Hence, we consider that JS-hADSC treatment can regulate autophagy to maintain a healthy cellular environment in Dox-challenged H9c2 cells.

Growth factor secretion by mesenchymal stem cells regulates various signaling pathways, such as the IGF1-IGF1R-AKT-mTOR pathway [59]. Our *in vitro* studies provided strong evidence that JS enhanced the migratory ability of hADSCs after treatment in a dose-dependent manner, which indicates the migration efficiency of the stem cells after transplantation. The damaged myocardial tissue secretes SDF1a, which helps to recruit stem cells via the chemokine marker CXCR4 to repair vascular damage [60, 61]. Several studies have focused on the paracrine activity of mesenchymal stem cells to mitigate vascular damage after stress [62–64]. ADSCs have the potential to secrete several growth factors, anti-inflammatory cytokines, and chemokines that mediate cardiac injury repair. These secreted soluble trophic factors promote migration, cell proliferation, and cytoprotection. Under pathological conditions, stem cells provide a supportive microenvironment by producing antioxidant and antiapoptotic factors to nourish the damaged cells [65]. Mesenchymal stem cells also secrete anti-fibrotic and angiogenic factors that modulate protection of the heart [66]. These pleotropic growth factors, such as VEGF, HGF, IGF, and PDGF, enhance

cardiac repair during chronic stress conditions (e.g., pathological hypertrophy). Various preconditioning mechanisms have been applied to enhance the ability of these growth factors to restore blood flow during damaged conditions such as myocardial infarction and pathological hypertension. Here, we used JS-preconditioned hADSCs, and examined their cardioprotective capabilities in both *in vitro* and *in vivo* contexts. The paracrine effects of JS-preconditioned hADSCs involve promoting a healthy microenvironment that protects H9c2 cells against the stress mediator doxorubicin. Based on our results, we hypothesized that ADSCs treated with JS act in a paracrine manner to exert a cardioprotective effect against Dox-induced cardiac damage that leads to enhanced EF (%) and FS (%) functions.

CONCLUSIONS

In this study, we reported that JS-preconditioned hADSCs have exhibited protective effects in dox-induced hypertrophic conditions in both *in vitro* and *in vivo* conditions (Figure 6). The *in vitro* model demonstrated that JS-preconditioned hADSCs has cardioprotective effects by regulating mitochondrial ROS, cardiac hypertrophy, and apoptosis in Dox-challenged H9c2 cells via activation of autophagy. Our *in vivo* data suggest that the preconditioning of hADSCs enhance cardiac function that might be regulated by

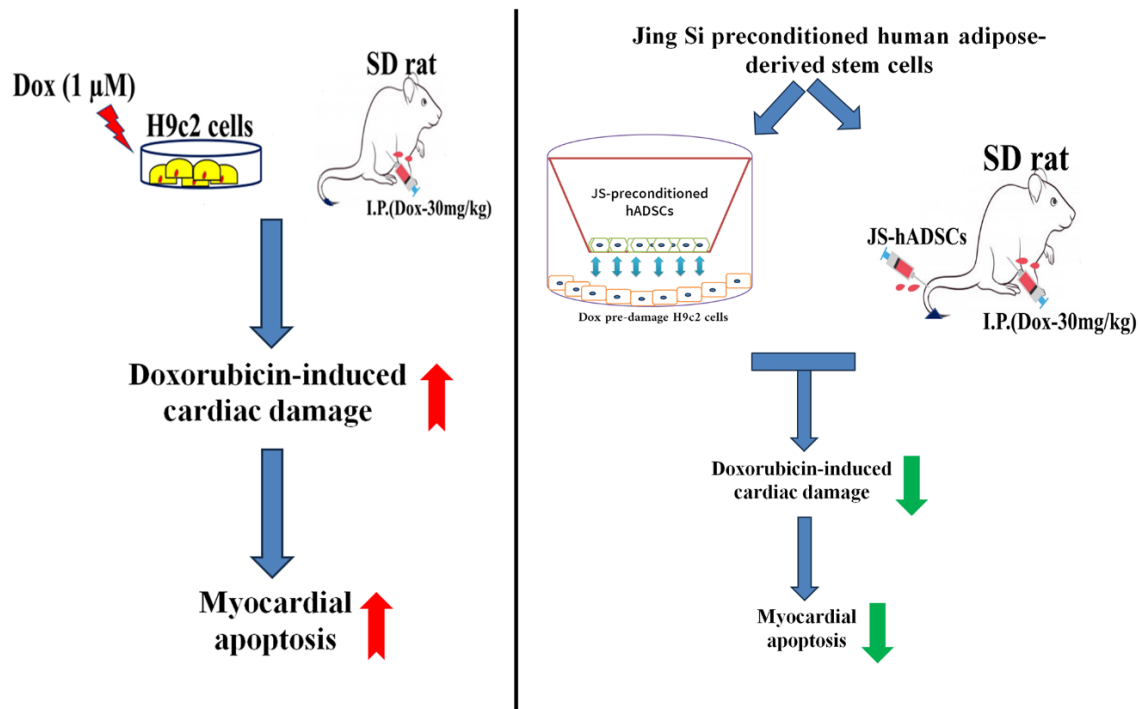


Figure 6. Graphical representation of the cardioprotective effects of Jing Shi and Jing Shi-preconditioned human adipose-derived stem cells (hADSCs) against Doxorubicin (Dox) induction in *in vitro* and *in vivo* models.

secreting growth factors and regulating cell viability, as well as improving migration efficiency. Taken together, our data indicate that JS preconditioning of hADSCs augments their cardioprotective effects in reducing ROS and apoptosis in H9c2 cells. To maintain the viability after transplantation is a greater challenge in stem cell therapy. So, we presume that this therapeutic strategy can also enhance cardiac function by enhancing the viability and migratory ability of the cells against Dox damage conditions. Our study shows that JS-preconditioned stem cells regulate the cardioprotective mechanism, both *in vitro* and *in vivo*, and these results suggest that this therapeutic approach is important for further investigation as a regenerative therapy.

Abbreviations

CHM: Chinese herbal medicine; Dox: doxorubicin; EF: ejection fraction; FS: fractional shortening; hADSCs: human adipose-derived stem cells; JS: novel herbal formulation Jing Si; JS-preconditioned hADSCs: Jing Shi-preconditioned human adipose-derived stem cells; SD: Sprague Dawley rat.

AUTHOR CONTRIBUTIONS

Dennis Jine-Yuan Hsieh and Chih-Yang Huang conceptualized and designed the study. Marthandam Asokan Shibu and Parthasarathi Barik collected and assembled the data. Chia-Hua Kuo, Cheng-Yen Shih, and Dennis Jine-Yuan Hsieh provided materials for the study. Bruce Chi-Kang Tsai, Parthasarathi Barik and Marthandam Asokan Shibu analyzed and interpreted the data. Bruce Chi-Kang Tsai and Parthasarathi Barik wrote the draft of the manuscript. Wei-Wen Kuo and Bruce Chi-Kang Tsai reviewed and gave the final approval of the manuscript. Pi-Yu Lin, Shinn-Zong Lin and Chih-Yang Huang provided the administrative support. Pi-Yu Lin, Cheng-Yen Shih, Shinn-Zong Lin, Tsung-Jung Ho, and Chih-Yang Huang provided financial support. All authors agree to be accountable for all aspects of work ensuring integrity and accuracy. All authors reviewed the manuscript.

ETHICAL STATEMENT

Animal experiments were approved by the Institutional Animal Care and Use Committee (IACUC, No. 108-70) of Tzu-Chi University Animal Care Center, Hualien, Taiwan. All experimental rats were maintained following the Animal Ethics Guidelines of Tzu-Chi University and all animals care followed Guide for the Care and Use of Laboratory Animals from National Institutes of Health.

CONFLICTS OF INTEREST

The authors declare that they have no conflicts of interest.

FUNDING

This study was funded by China Medical University (CMU103-TC-03), and Asia University grants (CMU102-AISA-04-08), and Hualien Tzu Chi Hospital grant (IMAR110-01-13), Taiwan.

REFERENCES

1. Roth GA, Johnson C, Abajobir A, Abd-Allah F, Abera SF, Abyu G, Ahmed M, Aksut B, Alam T, Alam K, Alla F, Alvis-Guzman N, Amrock S, et al. Global, Regional, and National Burden of Cardiovascular Diseases for 10 Causes, 1990 to 2015. *J Am Coll Cardiol.* 2017; 70:1–25.
<https://doi.org/10.1016/j.jacc.2017.04.052>
PMID:[28527533](https://pubmed.ncbi.nlm.nih.gov/28527533/)
2. Stults-Kolehmainen MA, Sinha R. The effects of stress on physical activity and exercise. *Sports Med.* 2014; 44:81–121.
<https://doi.org/10.1007/s40279-013-0090-5>
PMID:[24030837](https://pubmed.ncbi.nlm.nih.gov/24030837/)
3. Coats AJS. Ageing, demographics, and heart failure. *Eur Heart J Suppl.* 2019 (Suppl L); 21:L4–L7.
<https://doi.org/10.1093/eurheartj/suz235>
PMID:[31885504](https://pubmed.ncbi.nlm.nih.gov/31885504/)
4. Slivnick J, Lampert BC. Hypertension and Heart Failure. *Heart Fail Clin.* 2019; 15:531–41.
<https://doi.org/10.1016/j.hfc.2019.06.007>
PMID:[31472888](https://pubmed.ncbi.nlm.nih.gov/31472888/)
5. Bornstein AB, Rao SS, Marwaha K. Left Ventricular Hypertrophy. In: *StatPearls.* Treasure Island (FL): StatPearls Publishing. 2023.
PMID:[32491466](https://pubmed.ncbi.nlm.nih.gov/32491466/)
6. Fu X, Eggert M, Yoo S, Patel N, Zhong J, Steinke I, Govindarajulu M, Turumtay EA, Mouli S, Panizzi P, Beyers R, Denney T, Arnold R, Amin RH. The Cardioprotective Mechanism of Phenylaminoethyl Selenides (PAESe) Against Doxorubicin-Induced Cardiotoxicity Involves Frataxin. *Front Pharmacol.* 2021; 11:574656.
<https://doi.org/10.3389/fphar.2020.574656>
PMID:[33912028](https://pubmed.ncbi.nlm.nih.gov/33912028/)
7. Pandey S, Kuo WW, Ho TJ, Yeh YL, Shen CY, Chen RJ, Chang RL, Pai PY, Padma VV, Huang CY, Huang CY. Upregulation of IGF-1Rα intensifies doxorubicin-induced cardiac damage. *J Cell Biochem.* 2019; 120:16956–66.

- <https://doi.org/10.1002/jcb.28957>
PMID:[31104312](https://pubmed.ncbi.nlm.nih.gov/31104312/)
8. Leung WS, Kuo WW, Ju DT, Wang TD, Shao-Tsu Chen W, Ho TJ, Lin YM, Mahalakshmi B, Lin JY, Huang CY. Protective effects of diallyl trisulfide (DATS) against doxorubicin-induced inflammation and oxidative stress in the brain of rats. *Free Radic Biol Med*. 2020; 160:141–8.
<https://doi.org/10.1016/j.freeradbiomed.2020.07.018>
PMID:[32745770](https://pubmed.ncbi.nlm.nih.gov/32745770/)
 9. Bharathi Priya L, Baskaran R, Huang CY, Vijaya Padma V. Neferine modulates IGF-1R/Nrf2 signaling in doxorubicin treated H9c2 cardiomyoblasts. *J Cell Biochem*. 2018; 119:1441–52.
<https://doi.org/10.1002/jcb.26305>
PMID:[28731223](https://pubmed.ncbi.nlm.nih.gov/28731223/)
 10. Münzel T, Camici GG, Maack C, Bonetti NR, Fuster V, Kovacic JC. Impact of Oxidative Stress on the Heart and Vasculature: Part 2 of a 3-Part Series. *J Am Coll Cardiol*. 2017; 70:212–29.
<https://doi.org/10.1016/j.jacc.2017.05.035>
PMID:[28683969](https://pubmed.ncbi.nlm.nih.gov/28683969/)
 11. Moreira AC, Branco AF, Sampaio SF, Cunha-Oliveira T, Martins TR, Holy J, Oliveira PJ, Sardão VA. Mitochondrial apoptosis-inducing factor is involved in doxorubicin-induced toxicity on H9c2 cardiomyoblasts. *Biochim Biophys Acta*. 2014; 1842:2468–78.
<https://doi.org/10.1016/j.bbadis.2014.09.015>
PMID:[25283819](https://pubmed.ncbi.nlm.nih.gov/25283819/)
 12. Guo RM, Xu WM, Lin JC, Mo LQ, Hua XX, Chen PX, Wu K, Zheng DD, Feng JQ. Activation of the p38 MAPK/NF- κ B pathway contributes to doxorubicin-induced inflammation and cytotoxicity in H9c2 cardiac cells. *Mol Med Rep*. 2013; 8:603–8.
<https://doi.org/10.3892/mmr.2013.1554>
PMID:[23807148](https://pubmed.ncbi.nlm.nih.gov/23807148/)
 13. Sardão VA, Oliveira PJ, Holy J, Oliveira CR, Wallace KB. Doxorubicin-induced mitochondrial dysfunction is secondary to nuclear p53 activation in H9c2 cardiomyoblasts. *Cancer Chemother Pharmacol*. 2009; 64:811–27.
<https://doi.org/10.1007/s00280-009-0932-x>
PMID:[19184017](https://pubmed.ncbi.nlm.nih.gov/19184017/)
 14. Cyranoski D. Why Chinese medicine is heading for clinics around the world. *Nature*. 2018; 561:448–50.
<https://doi.org/10.1038/d41586-018-06782-7>
PMID:[30258149](https://pubmed.ncbi.nlm.nih.gov/30258149/)
 15. Tang JL, Hackshaw A, Lao LX, Liu BY, Chung VC. Improving research on the efficacy, effectiveness, and harms of traditional chinese medicine. *Evid Based Complement Alternat Med*. 2014; 2014:657679.
<https://doi.org/10.1155/2014/657679> PMID:[25587345](https://pubmed.ncbi.nlm.nih.gov/25587345/)
 16. Wong W, Lam LK, Li R, Ho SH, Fai LK, Li Z. A comparison of the effectiveness between Western medicine and Chinese medicine outpatient consultations in primary care. *Complement Ther Med*. 2011; 19:264–75.
<https://doi.org/10.1016/j.ctim.2011.07.001>
PMID:[21944656](https://pubmed.ncbi.nlm.nih.gov/21944656/)
 17. Wang WJ, Zhang T. Integration of traditional Chinese medicine and Western medicine in the era of precision medicine. *J Integr Med*. 2017; 15:1–7.
[https://doi.org/10.1016/S2095-4964\(17\)60314-5](https://doi.org/10.1016/S2095-4964(17)60314-5)
PMID:[28088253](https://pubmed.ncbi.nlm.nih.gov/28088253/)
 18. Yang Y, Islam MS, Wang J, Li Y, Chen X. Traditional Chinese Medicine in the Treatment of Patients Infected with 2019-New Coronavirus (SARS-CoV-2): A Review and Perspective. *Int J Biol Sci*. 2020; 16:1708–17.
<https://doi.org/10.7150/ijbs.45538>
PMID:[32226288](https://pubmed.ncbi.nlm.nih.gov/32226288/)
 19. Shibu MA, Lin YJ, Chiang CY, Lu CY, Goswami D, Sundhar N, Agarwal S, Islam MN, Lin PY, Lin SZ, Ho TJ, Tsai WT, Kuo WW, Huang CY. Novel anti-aging herbal formulation Jing Si displays pleiotropic effects against aging associated disorders. *Biomed Pharmacother*. 2022; 146:112427.
<https://doi.org/10.1016/j.biopha.2021.112427>
PMID:[35062051](https://pubmed.ncbi.nlm.nih.gov/35062051/)
 20. Guo Y, Yu Y, Hu S, Chen Y, Shen Z. The therapeutic potential of mesenchymal stem cells for cardiovascular diseases. *Cell Death Dis*. 2020; 11:349.
<https://doi.org/10.1038/s41419-020-2542-9>
PMID:[32393744](https://pubmed.ncbi.nlm.nih.gov/32393744/)
 21. Pittenger MF, Discher DE, Péault BM, Phinney DG, Hare JM, Caplan AI. Mesenchymal stem cell perspective: cell biology to clinical progress. *NPJ Regen Med*. 2019; 4:22.
<https://doi.org/10.1038/s41536-019-0083-6>
PMID:[31815001](https://pubmed.ncbi.nlm.nih.gov/31815001/)
 22. Mazini L, Rochette L, Amine M, Malka G. Regenerative Capacity of Adipose Derived Stem Cells (ADSCs), Comparison with Mesenchymal Stem Cells (MSCs). *Int J Mol Sci*. 2019; 20:2523.
<https://doi.org/10.3390/ijms20102523>
PMID:[31121953](https://pubmed.ncbi.nlm.nih.gov/31121953/)
 23. Mazini L, Ezzoubi M, Malka G. Overview of current adipose-derived stem cell (ADSCs) processing involved in therapeutic advancements: flow chart and regulation updates before and after COVID-19. *Stem Cell Res Ther*. 2021; 12:1.
<https://doi.org/10.1186/s13287-020-02006-w>
PMID:[33397467](https://pubmed.ncbi.nlm.nih.gov/33397467/)
 24. Rochette L, Mazini L, Malka G, Zeller M, Cottin Y, Vergely C. The Crosstalk of Adipose-Derived Stem Cells (ADSC), Oxidative Stress, and Inflammation in

- Protective and Adaptive Responses. *Int J Mol Sci.* 2020; 21:9262.
<https://doi.org/10.3390/ijms21239262>
PMID:[33291664](https://pubmed.ncbi.nlm.nih.gov/33291664/)
25. Trzyna A, Banaś-Ząbczyk A. Adipose-Derived Stem Cells Secretome and Its Potential Application in “Stem Cell-Free Therapy”. *Biomolecules.* 2021; 11:878.
<https://doi.org/10.3390/biom11060878>
PMID:[34199330](https://pubmed.ncbi.nlm.nih.gov/34199330/)
26. Lee PY, Tsai BCK, Sitorus MA, Lin PY, Lin SZ, Shih CY, Lu SY, Lin YM, Ho TJ, Huang CY. Ohwia caudata aqueous extract attenuates doxorubicin-induced mitochondrial dysfunction in Wharton’s jelly-derived mesenchymal stem cells. *Environ Toxicol.* 2023. [Epub ahead of print].
<https://doi.org/10.1002/tox.23880> PMID:[37461261](https://pubmed.ncbi.nlm.nih.gov/37461261/)
27. Liu SP, Shibu MA, Tsai FJ, Hsu YM, Tsai CH, Chung JG, Yang JS, Tang CH, Wang S, Li Q, Huang CY. Tetramethylpyrazine reverses high-glucose induced hypoxic effects by negatively regulating HIF-1 α induced BNIP3 expression to ameliorate H9c2 cardiomyoblast apoptosis. *Nutr Metab (Lond).* 2020; 17:12.
<https://doi.org/10.1186/s12986-020-0432-x>
PMID:[32021640](https://pubmed.ncbi.nlm.nih.gov/32021640/)
28. Barik P, Shibu MA, Hsieh DJ, Day CH, Chen RJ, Kuo WW, Chang YM, Padma VV, Ho TJ, Huang CY. Cardioprotective effects of transplanted adipose-derived stem cells under Ang II stress with Danggui administration augments cardiac function through upregulation of insulin-like growth factor 1 receptor in late-stage hypertension rats. *Environ Toxicol.* 2021; 36:1466–75.
<https://doi.org/10.1002/tox.23145> PMID:[33881220](https://pubmed.ncbi.nlm.nih.gov/33881220/)
29. Chang WS, Tsai CW, Yang JS, Hsu YM, Shih LC, Chiu HY, Bau DT, Tsai FJ. Resveratrol inhibited the metastatic behaviors of cisplatin-resistant human oral cancer cells via phosphorylation of ERK/p-38 and suppression of MMP-2/9. *J Food Biochem.* 2021; 45:e13666.
<https://doi.org/10.1111/jfbc.13666> PMID:[34008860](https://pubmed.ncbi.nlm.nih.gov/34008860/)
30. Cheng FJ, Huynh TK, Yang CS, Hu DW, Shen YC, Tu CY, Wu YC, Tang CH, Huang WC, Chen Y, Ho CY. Hesperidin Is a Potential Inhibitor against SARS-CoV-2 Infection. *Nutrients.* 2021; 13:2800.
<https://doi.org/10.3390/nu13082800>
PMID:[34444960](https://pubmed.ncbi.nlm.nih.gov/34444960/)
31. Lin JY, Ho TJ, Tsai BCK, Chiang CY, Kao HC, Kuo WW, Chen RJ, Viswanadha VP, Huang CW, Huang CY. Exercise renovates H2S and Nrf2-related antioxidant pathways to suppress apoptosis in the natural ageing process of male rat cortex. *Biogerontology.* 2021; 22:495–506.
<https://doi.org/10.1007/s10522-021-09929-8>
PMID:[34251569](https://pubmed.ncbi.nlm.nih.gov/34251569/)
32. Lin WY, Tsai BCK, Day CH, Chiu PL, Chen RJ, Chen MYC, Padma VV, Luk HN, Lee HC, Huang CY. Arecoline induces heart injure via Fas/Fas ligand apoptotic pathway in heart of Sprague-Dawley rat. *Environ Toxicol.* 2021; 36:1567–75.
<https://doi.org/10.1002/tox.23153> PMID:[33929070](https://pubmed.ncbi.nlm.nih.gov/33929070/)
33. Tsai BCK, Kuo WW, Day CH, Hsieh DJY, Kuo CH, Daddam J, Chen RJ, Padma VV, Wang G, Huang CY. The soybean bioactive peptide VHVV alleviates hypertension-induced renal damage in hypertensive rats via the SIRT1-PGC1 α /Nrf2 pathway. *Journal of Functional Foods.* 2020; 75:104255.
<https://doi.org/10.1016/j.jff.2020.104255>
34. Wang ZH. Anti-glycative effects of asiatic acid in human keratinocyte cells. *Biomedicine (Taipei).* 2014; 4:19.
<https://doi.org/10.7603/s40681-014-0019-9>
PMID:[25520932](https://pubmed.ncbi.nlm.nih.gov/25520932/)
35. Chiu WC, Yang HH, Chiang SC, Chou YX, Yang HT. Auricularia polytricha aqueous extract supplementation decreases hepatic lipid accumulation and improves antioxidative status in animal model of nonalcoholic fatty liver. *Biomedicine (Taipei).* 2014; 4:12.
<https://doi.org/10.7603/s40681-014-0012-3>
PMID:[25520925](https://pubmed.ncbi.nlm.nih.gov/25520925/)
36. Lu SY, Tsai BCK, Van Thao D, Lai CH, Chen MYC, Kuo WW, Kuo CH, Lin KH, Hsieh DJY, Huang CY. Cardiac-specific overexpression of insulin-like growth factor II receptor- α interferes with the regulation of calcium homeostasis in the heart under hyperglycemic conditions. *Mol Biol Rep.* 2023; 50:4329–38.
<https://doi.org/10.1007/s11033-023-08327-2>
PMID:[36928640](https://pubmed.ncbi.nlm.nih.gov/36928640/)
37. Arroyo JP, Schweickert AJ. Back to basics in physiology: fluids in the renal and cardiovascular systems: Academic Press). 2013.
38. Chiang CJ, Tsai BCK, Lu TL, Chao YP, Day CH, Ho TJ, Wang PN, Lin SC, Padma VV, Kuo WW, Huang CY. Diabetes-induced cardiomyopathy is ameliorated by heat-killed Lactobacillus reuteri GMNL-263 in diabetic rats via the repression of the toll-like receptor 4 pathway. *Eur J Nutr.* 2021; 60:3211–23.
<https://doi.org/10.1007/s00394-020-02474-z>
PMID:[33555373](https://pubmed.ncbi.nlm.nih.gov/33555373/)
39. Ho TJ, Chi-Kang Tsai B, Kuo CH, Luk HN, Day CH, Jine-Yuan Hsieh D, Chen RJ, Kuo WW, Kumar VB, Yao CH, Huang CY. Arecoline induces cardiotoxicity by upregulating and activating cardiac hypertrophy-related pathways in Sprague-Dawley rats. *Chem Biol Interact.* 2022; 354:109810.
<https://doi.org/10.1016/j.cbi.2022.109810>
PMID:[34999050](https://pubmed.ncbi.nlm.nih.gov/34999050/)
40. Lin CC, Chen KB, Tsai CH, Tsai FJ, Huang CY, Tang CH, Yang JS, Hsu YM, Peng SF, Chung JG. Casticin inhibits

- human prostate cancer DU 145 cell migration and invasion via Ras/Akt/NF- κ B signaling pathways. *J Food Biochem*. 2019; 43:e12902.
<https://doi.org/10.1111/jfbc.12902> PMID:31353708
41. Das G, Shrivage BV, Baehrecke EH. Regulation and function of autophagy during cell survival and cell death. *Cold Spring Harb Perspect Biol*. 2012; 4:a008813.
<https://doi.org/10.1101/cshperspect.a008813>
PMID:22661635
42. Priya LB, Baskaran R, Huang CY, Padma VV. Neferine ameliorates cardiomyoblast apoptosis induced by doxorubicin: possible role in modulating NADPH oxidase/ROS-mediated NF κ B redox signaling cascade. *Sci Rep*. 2017; 7:12283.
<https://doi.org/10.1038/s41598-017-12060-9>
PMID:28947826
43. Christidi E, Brunham LR. Regulated cell death pathways in doxorubicin-induced cardiotoxicity. *Cell Death Dis*. 2021; 12:339.
<https://doi.org/10.1038/s41419-021-03614-x>
PMID:33795647
44. Huang CY, Kuo WW, Lo JF, Ho TJ, Pai PY, Chiang SF, Chen PY, Tsai FJ, Tsai CH, Huang CY. Doxorubicin attenuates CHIP-guarded HSF1 nuclear translocation and protein stability to trigger IGF-IIR-dependent cardiomyocyte death. *Cell Death Dis*. 2016; 7:e2455.
<https://doi.org/10.1038/cddis.2016.356>
PMID:27809308
45. Cappetta D, De Angelis A, Sapio L, Prezioso L, Illiano M, Quaini F, Rossi F, Berrino L, Naviglio S, Urbanek K. Oxidative Stress and Cellular Response to Doxorubicin: A Common Factor in the Complex Milieu of Anthracycline Cardiotoxicity. *Oxid Med Cell Longev*. 2017; 2017:1521020.
<https://doi.org/10.1155/2017/1521020>
PMID:29181122
46. Hu C, Zhang X, Wei W, Zhang N, Wu H, Ma Z, Li L, Deng W, Tang Q. Matrine attenuates oxidative stress and cardiomyocyte apoptosis in doxorubicin-induced cardiotoxicity via maintaining AMPK α /UCP2 pathway. *Acta Pharm Sin B*. 2019; 9:690–701.
<https://doi.org/10.1016/j.apsb.2019.03.003>
PMID:31384530
47. Chen TS, Chuang SY, Shen CY, Ho TJ, Chang RL, Yeh YL, Kuo CH, Mahalakshmi B, Kuo WW, Huang CY. Antioxidant Sirt1/Akt axis expression in resveratrol pretreated adipose-derived stem cells increases regenerative capability in a rat model with cardiomyopathy induced by diabetes mellitus. *J Cell Physiol*. 2021; 236:4290–302.
<https://doi.org/10.1002/jcp.30057>
PMID:33421145
48. Chang YM, Shibu MA, Chen CS, Tamilselvi S, Tsai CT, Tsai CC, Kumar KA, Lin HJ, Mahalakshmi B, Kuo WW, Huang CY. Adipose derived mesenchymal stem cells along with *Alpinia oxyphylla* extract alleviate mitochondria-mediated cardiac apoptosis in aging models and cardiac function in aging rats. *J Ethnopharmacol*. 2021; 264:113297.
<https://doi.org/10.1016/j.jep.2020.113297>
PMID:32841691
49. Guo D, Ying Z, Wang H, Chen D, Gao F, Ren H, Wang G. Regulation of autophagic flux by CHIP. *Neurosci Bull*. 2015; 31:469–79.
<https://doi.org/10.1007/s12264-015-1543-7>
PMID:26219223
50. Sishi BJ, Loos B, van Rooyen J, Engelbrecht AM. Autophagy upregulation promotes survival and attenuates doxorubicin-induced cardiotoxicity. *Biochem Pharmacol*. 2013; 85:124–34.
<https://doi.org/10.1016/j.bcp.2012.10.005>
PMID:23107818
51. Pandey S, Kuo WW, Shen CY, Yeh YL, Ho TJ, Chen RJ, Chang RL, Pai PY, Viswanadha VP, Huang CY, Huang CY. Insulin-like growth factor II receptor- α is a novel stress-inducible contributor to cardiac damage underpinning doxorubicin-induced oxidative stress and perturbed mitochondrial autophagy. *Am J Physiol Cell Physiol*. 2019; 317:C235–43.
<https://doi.org/10.1152/ajpcell.00079.2019>
PMID:31116582
52. Murrow L, Debnath J. Autophagy as a stress-response and quality-control mechanism: implications for cell injury and human disease. *Annu Rev Pathol*. 2013; 8:105–37.
<https://doi.org/10.1146/annurev-pathol-020712-163918> PMID:23072311
53. Bang S, Kaur S, Kurokawa M. Regulation of the p53 Family Proteins by the Ubiquitin Proteasomal Pathway. *Int J Mol Sci*. 2019; 21:261.
<https://doi.org/10.3390/ijms21010261>
PMID:31905981
54. Xu H, Yu W, Sun S, Li C, Zhang Y, Ren J. Luteolin Attenuates Doxorubicin-Induced Cardiotoxicity Through Promoting Mitochondrial Autophagy. *Front Physiol*. 2020; 11:113.
<https://doi.org/10.3389/fphys.2020.00113>
PMID:32116805
55. Ramanathan A, Schreiber SL. Direct control of mitochondrial function by mTOR. *Proc Natl Acad Sci USA*. 2009; 106:22229–32.
<https://doi.org/10.1073/pnas.0912074106>
PMID:20080789
56. Lizama BN, Palubinsky AM, Raveendran VA, Moore AM, Federspiel JD, Codreanu SG, Liebler DC,

- McLaughlin B. Neuronal Preconditioning Requires the Mitophagic Activity of C-terminus of HSC70-Interacting Protein. *J Neurosci*. 2018; 38:6825–40.
<https://doi.org/10.1523/JNEUROSCI.0699-18.2018>
PMID:[29934347](https://pubmed.ncbi.nlm.nih.gov/29934347/)
57. Hoshino A, Mita Y, Okawa Y, Ariyoshi M, Iwai-Kanai E, Ueyama T, Ikeda K, Ogata T, Matoba S. Cytosolic p53 inhibits Parkin-mediated mitophagy and promotes mitochondrial dysfunction in the mouse heart. *Nat Commun*. 2013; 4:2308.
<https://doi.org/10.1038/ncomms3308> PMID:[23917356](https://pubmed.ncbi.nlm.nih.gov/23917356/)
58. Schaaf MB, Keulers TG, Vooijs MA, Rouschop KM. LC3/GABARAP family proteins: autophagy-(un)related functions. *FASEB J*. 2016; 30:3961–78.
<https://doi.org/10.1096/fj.201600698R>
PMID:[27601442](https://pubmed.ncbi.nlm.nih.gov/27601442/)
59. Chen PC, Kuo YC, Chuong CM, Huang YH. Niche Modulation of IGF-1R Signaling: Its Role in Stem Cell Pluripotency, Cancer Reprogramming, and Therapeutic Applications. *Front Cell Dev Biol*. 2021; 8:625943.
<https://doi.org/10.3389/fcell.2020.625943>
PMID:[33511137](https://pubmed.ncbi.nlm.nih.gov/33511137/)
60. Chen H, Li G, Liu Y, Ji S, Li Y, Xiang J, Zhou L, Gao H, Zhang W, Sun X, Fu X, Li B. Pleiotropic Roles of CXCR4 in Wound Repair and Regeneration. *Front Immunol*. 2021; 12:668758.
<https://doi.org/10.3389/fimmu.2021.668758>
PMID:[34122427](https://pubmed.ncbi.nlm.nih.gov/34122427/)
61. Cencioni C, Capogrossi MC, Napolitano M. The SDF-1/CXCR4 axis in stem cell preconditioning. *Cardiovasc Res*. 2012; 94:400–7.
<https://doi.org/10.1093/cvr/cvs132>
PMID:[22451511](https://pubmed.ncbi.nlm.nih.gov/22451511/)
62. Pankajakshan D, Agrawal DK. Mesenchymal Stem Cell Paracrine Factors in Vascular Repair and Regeneration *J Biomed Technol Res*. 2014; 1:10.19104.
<https://doi.org/10.19104/jbtr.2014.107>
PMID:[28890954](https://pubmed.ncbi.nlm.nih.gov/28890954/)
63. Xu H, Lee CW, Wang YF, Huang S, Shin LY, Wang YH, Wan Z, Zhu X, Yung PSH, Lee OK. The Role of Paracrine Regulation of Mesenchymal Stem Cells in the Crosstalk With Macrophages in Musculoskeletal Diseases: A Systematic Review. *Front Bioeng Biotechnol*. 2020; 8:587052.
<https://doi.org/10.3389/fbioe.2020.587052>
PMID:[33324622](https://pubmed.ncbi.nlm.nih.gov/33324622/)
64. Gnecci M, Zhang Z, Ni A, Dzau VJ. Paracrine mechanisms in adult stem cell signaling and therapy. *Circ Res*. 2008; 103:1204–19.
<https://doi.org/10.1161/CIRCRESAHA.108.176826>
PMID:[19028920](https://pubmed.ncbi.nlm.nih.gov/19028920/)
65. Chen F, Liu Y, Wong NK, Xiao J, So KF. Oxidative Stress in Stem Cell Aging. *Cell Transplant*. 2017; 26:1483–95.
<https://doi.org/10.1177/0963689717735407>
PMID:[29113471](https://pubmed.ncbi.nlm.nih.gov/29113471/)
66. Baraniak PR, McDevitt TC. Stem cell paracrine actions and tissue regeneration. *Regen Med*. 2010; 5:121–43.
<https://doi.org/10.2217/rme.09.74>
PMID:[20017699](https://pubmed.ncbi.nlm.nih.gov/20017699/)